New Materials, Compounds and Applications
Vol.9, No.3, 2025, pp.629-644
https://doi.org/10.62476/nmca.93629

SYNTHESIS AND SPECTROSCOPIC CHARACTERIZATION OF La(III), Eu(III) AND Ni(II) COMPLEXES WITH ENAMINE LIGANDS DERIVED FROM 4,4,4-TRIFLUORO-1-(2-FURYL)-1,3-BUTANEDIONE

Heba Salah, Jassim Abbas AL-Hilifi*

Department of Chemistry, College of Science, University of Misan, Maysan, Iraq

Abstract. Interaction of nickel metal and two lanthanide metals, lanthanum (La) and europium (Eu), with two enamine compounds prepared from furyltrifluoroacetate with methylamine and aniline, formed six different complexes. The metal of the third transition chain is nickel metal and two metals of lanthanides, namely lanthanum and europium, through their interaction with two enamine compounds prepared from the interaction of furyltrifluoroacetate with methylamine and aniline as a result of these interactions formed six complexes, four of which have the characteristics of diamagnetic for complexes prepared from metals lanthanum and nickel and their hybridization is d^2sp^3 and dsp^2 respectively and paramagnetic for complexes prepared from europium hybridization d^2sp^3 with the survival of electrons Isolated in the orbital f, causing the complexes to be paramagnetic according to magnetic susceptibility measurements. According to the electrical conductivity measurements, no ions are outside the coordination sphere. The electrical conductivity measurements show no ions outside the coordinate sphere. Hence, the bond is in the form of a covalent coordinate bond between the oxygen atom and the metals to which it is bonded, i.e., the charge of the oxygen atom equalizes the metal charge. The measurements of I.R. spectra prove this after comparing the spectra of enamine compounds with the complexes prepared from them, while the nitrogen atom is connected to the metals by a donor coordinate bond, i.e., the hydrogen atom remains attached to it in the complexes. After the preparation of amine compounds, a great controversy emerged during the diagnosis of compounds, which was to determine which oxygen atoms were replaced by a nitrogen atom. After preparation, many isomers appeared, so it required the diagnosis of compounds prepared with several NMR measurements, namely ^{1}H NMR, ^{13}C NMR, ^{19}F NMR, ^{15}N NMR, HSQC, HMBC, COSY, DEPT135. After these measurements, the prepared amine compounds and the complexes prepared from them were characterized.

Keywords: *Furyltrifluoroacetone, lanthanum, europium, nickel, spectroscopic characterizations, NMR, IR.*

Corresponding Author: *Jassim Abbas AL-Hilifi, Department of Chemistry, College of Science, University of Misan, Maysan, Iraq, e-mail: Jassimal-hilfi@uomisan.edu.iq*

Received: *9 June 2025;* ***Accepted:*** *30 September 2025;* ***Published:*** *4 December 2025.*

1. Introduction

Complexes formed from beta-diketone ligands containing a CF_3 group with metals, especially from the lanthanide group, have three distinctive uses: the first is in the preparation of new ligands and their reaction with certain metals to prepare new complexes (Hanson, 2014). The second use is in the industry due to their ability to luminesce and the third use is in separation and extraction, as beta-diketone compounds containing the CF_3 group can chelate selectively with lanthanide metals, allowing for separation (Arrachart *et al*., 2021). The beta-diketone hexafluoroacetylacetone compound forms complexes with metals, forming a bidentate complex in the final form. It reacts

with hydrazine and forms new compounds, such as pyrazoles, acting as donor ligands for one donor when they react with metals in the new complexes (AL-Hilfi *et al*., 2020).

Omoregie, H.O. prepared Nickel (II) complex of 4,4,4-trifluoro-1-(2-Naphthyl)-1,3-butanedione (tfnb) and its 2,2′-bipyridine, ethylenediamine and 1,10-phenanthroline adducts, which showed antimicrobial activity. The antimicrobial activity shows that [Ni(tfnb)2]2H_2O complex and its adducts have no antibacterial and antifungal activities (Omoregie, 2018). Mautner and his coleages have prepared a series of complexes in the form of large compounds composed of Samarium metal and the ligand 4,4,4-trifluoro 1-(naphthalene-2-yl)-1,3-butanedionate with a series of bipyridine ligands in the form of polypyridyl to use in the luminescence. A novel series of polypyridyl adducts, [Sm$(TFA)_3$(NN)] (2–4), with ntfa = 4,4,4-trifluoro 1-(naphthalene-2-yl)-1,3-butanedionate, NN = 2,2-bipyridine (bipy), 4,4-dimethyl-2,2-bipyridine (4,4-Me2bipy) and 5,5-dimethyl-2,2-bipyridine (5,5-Me2bipy) were synthesized from the precursor complex [Sm(ntfa)3$(MeOH)_2$] (1) and the corresponding pyridyl ligands. Single X-ray crystallography showed that the complexes displayed an 8-coordinated geometry. The solid pyridyl adducts 2-4 exhibited luminescence emission in the NIR and visible regions with close quantum yields (QY = 0.20–0.25 %) (Mautner *et al*., 2022). The 4,4,4-trifluoro-1-(biphenyl-4-yl),l ijuhbutane-1,3-dione (HL) and its complexation properties in solution were examined. Mixed ligand chelate extraction of light trivalent lanthanoids (La÷Gd) from chloride medium at constant ionic strength μ = 0.1 into C_6H_6 with HL in combination with one of the three phosphine oxide compounds, trioctylphosphine oxide (TOPO), tributylphosphine oxide (TBPO) or triphenylphosphine oxide (TPPO) was studied (Petrova, 2022). Taydakov et al. (2022) synthesized a binuclear complex from reacting Gadolinium (III) with 4,4,4-trifluoro-1-(1-methyl-1H-pyrazol-4-yl) butane-1,3-dione as a bidentate ligand, with two oxygen atoms, the ligand that has a negative charge and is in the form of an enol. A binuclear Gadolinium (III) complex was obtained through the interaction of $GdCl_3 \cdot 6H_2O$, 4,4,4-trifluoro-1-(1-methyl-1H-pyrazol-4-yl) butane-1,3-dione and NaOH in MeOH solution. The molar ratio of reagents equal to 1:3:3 was used. Upon recrystallization of wet 1,4-dioxane, an intermediate hydrated complex formed a stable crystalline solvate with the composition [$(Gd_2(L)3(H_2O))2(C_4H_8O_2)$] 2$(C_4H_8O_2)$ (Taydakov *et al*., 2022).

Recent advances show that coupling metal-center photophysics with in-situ-generated hybrid hosts can amplify signal read-out and environmental stability. For instance, a ZnO/asymmetric-dimer liquid-crystal nanohybrid displayed a two-fold boost in fluorescence quantum yield once the dimeric mesogen templated exciton migration across the oxide interface (Banoon *et al*., 2023a). Parallel mechanistic insight from the companion review on asymmetric dimeric liquid crystals highlights how π-stacked, shape-persistent cores funnel energy into metal-containing domains, creating highly efficient antennae for sensing and display technologies (Banoon *et al*., 2023b). Hybrid nano-architectures of ZnO and π-conjugated ligands have already shown tangible biomedical value. When a graphene-oxide/ZnO composite was loaded with doxorubicin it triggered selective apoptosis in HCT-116 colorectal cancer cells while shielding the drug from premature photolysis (Banoon & Ghasemian 2022). Surface-acoustic-wave microfluidics further broadens this biomedical window, it provides a high-throughput 3-D culture platform on which such nanohybrids can be evaluated (Alhasan *et al*., 2014). Similar cytocompatible behaviour was reported for bio-templated TiO_2 and chitosan-ZnO systems that curtailed *Bacillus licheniformis* growth and mitigated multidrug resistance (Ali *et al*., 2020; Aldujaili & Banoon, 2020). These precedents suggest that the ordered

dimer matrix explored here could be repurposed as an optical biosensor or a photo-responsive drug gate simply by exchanging the guest chromophore.

Beyond optical merit, sustainability considerations increasingly steer ligand and process selection. Bio-inspired degradation routes reported by Aziz et al. (2024) demonstrate how heteroatom-rich chelators can be sourced or recycled from low-value streams. Positioning our furyl-trifluoroacetylacetone framework within this green-chemistry paradigm may facilitate cradle-to-cradle recovery of both ligand and metal, especially once immobilised on oxide or polymer supports. Environmental stewardship provides a parallel driver for such multifunctional hybrids. In plastic-laden soils from the Maysan governorate, ZnO-bearing eco-coagulants and oil-degrading Bacillus consortia have already been field-tested as dual-action remediation tools (Saleh *et al*., 2021; Aziz *et al*., 2024). Embedding metal-organic antennae inside recyclable liquid-crystal hosts therefore aligns the present optical platform with United Nations SDG 12 on responsible production and consumption.

Accordingly, this study set out to prepare two previously unreported enamine derivatives of 4,4,4-trifluoro-1-(2-furyl)-1,3-butanedione, to isolate their stoichiometric La(III), Eu(III) and Ni(II) complexes and to unravel how each ligand binds, what coordination geometry emerges and how the electronic environment is altered, using a concerted suite of FT-IR, multinuclear NMR, UV–Vis, molar-conductivity and magnetic-susceptibility measurements. Clarifying these structure-property links broadens the coordination landscape of CF_3-β-diketone enamines and furnishes a platform for future exploration of their photonic, separation and catalytic promise.

2. Materials and Methods

Preparation of ligands

Two compounds, enamine (ligands) L1 and L2, derived from the condensation of the first amine methyl amine of the aliphatic compound and the second first amino aniline of the aromatic compound with beta-diketone 4,4,4-trifluoro-1-(2-fural)-3,1-butanedione (FTFA) were prepared as follows: according to the previous literature with some modifications (AL-Hilfi *et al*., 2015). Dissolve (2 mmol) of the beta-diketone compound in (5 ml) ethanol released in a glass flask of 100 ml, then add the primary amine (2 mmol) gradually dissolved in (5 ml) ethanol, then add to the resulting mixture (1ml) glacial acetic acid and leave the mix (24 hrs.) under the spiral Reflux at a temperature of 70°C, after the end of the reaction, leave the mixture to dry inside the oven at 37°C, then purify the product by recrystallization method using a blend of 30% ethanol, 70% n-hexane, then add the coal, then filter the solution, then leave the product to dry at 37°C (AL-Hilfi *et al*., 2020).

Ligand L1 preparation: reaction (0.4122 g) of FTFA with (0.1862 g) of aniline.

Ligand L2 preparation: reaction (0.4122 g) of FTFA with (0.0621 g) of methylamine.

Preparation of complexes

Mixing (0.32 m mol: 0.12 g) of $LaCl_3 \cdot 7H_2O$ or (0.31 m mol: 0.11 g) of $EuCl_3 \cdot 6H_2O$ dissolved in (5 ml) ethanol or (0.52 m mol: 0.12 g) of $NiCl_2 \cdot 6H_2O$ dissolved in (5 ml) deionized water with (0.98 m mol: 0.278 g) or (0.93 m mol: 0.26 g) or (1.04 m mol: 0.29 g) of ligand prepared in the first step and dissolved in (10 ml) ethanol and respectively in a mixing ratio of 1:3 for Lanthanum and Europium metals and by a mixing ratio 1:2 for

Nickel metal. The mixture is then refluxed at a temperature of 70 °C for 3 hours and left for 24 hours with magnetic stirring. Then add to the resulting mixture (5) sodium hydroxide drops at a concentration of 10% with (1 ml) deionized water and leave the product for 15 minutes to note the deposition of the solution, then filtered and then left in the oven at a temperature of 50 °C to dry. The solid product was purified by washing it with 50% ethanol (AL-Hilfi, 2020).

Mixing (0.38 m mol: 0.14 g) of $LaCl_3 \cdot 7H_2O$ or (0.31 m mol: 0.11 g) of $EuCl_3 \cdot 6H_2O$ dissolved in (5 mL) methanol or (0.43 m mol: 0.10 g) of $NiCl_2 \cdot 6H_2O$ dissolved in (5 ml) deionized water with (1.16 m mol: 0.25 g) or (0.96 m mol: 0.21 g) or (0.86 m mol: 0.19 g) of candle prepared in the first step and dissolved in (10 ml) methanol respectively in a mixing ratio of 1:3 for Lanthanum and Europium metals and a mixing ratio of 1:2 for nickel metal. Then, the mixture is refluxed at a temperature of 70 °C for 3 hours and left for 24 hours with magnetic stirring. Then add to the resulting mixture (5) sodium hydroxide drops at a concentration of 10% with (1 ml) deionized water and leave the product for 15 minutes to note the deposition of the solution, then filtered and then left in the oven at a temperature of 50 °C to dry. The product is purified by washing it with 50% ethanol (AL-Hilfi, 2015).

3. Results and Discussion

The synthetic Chemical formula of the prepared compounds with their nomenclature and symbols are shown in Table 1.

Table 1. Chemical formula, nomenclature and symbols of prepared compounds

Symbols of compound	Chemical formula	nomenclature
S	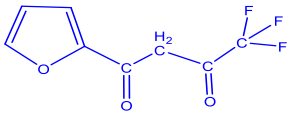	4,4,4-trifloro-1-(2-furyl)-1,3-butanedione
SLa	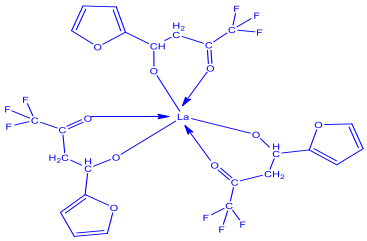	Tris(4,4,4-trifluoro-1-(furyl-2-yl)-3-oxobutoxy)lanthanum.
L1	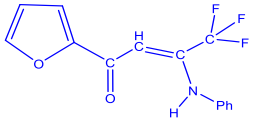	(Z)-4,4,4-trifluoro-1-(furan-2-yl)-3-(methylamino)but-2-en-1-one
L2	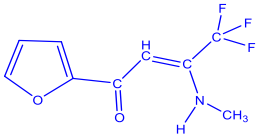	(Z)-4,4,4-trifluoro-1-(furan-2-yl)-3-(phenylamino)but-2-en-1-one

1-M=La, L=Ph
L1La

2-M=Eu, L=Ph
L1Eu

3-M=La,
L=Me
L2La

4-M=Eu,
L=Me
L2Eu

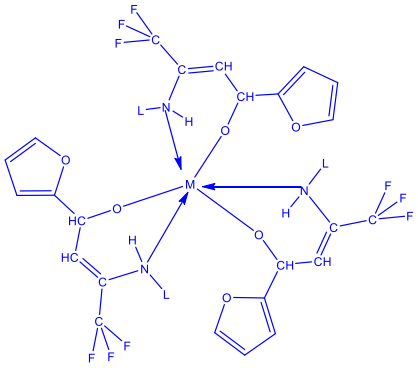

1-M=La, L=Ph
Tris(((Z)-4,4,4-trifluoro-1-(furan-2-yl)-3-(phenylamino)but-2-en-1-yl)oxy)Lanthanum
2-M=Eu, L=Ph
Tris(((Z)-4,4,4-trifluoro-1-(furan-2-yl)-3-(phenylamino)but-2-en-1-yl)oxy)Europium
3-M=La, L=Me
Tris(((Z)-4,4,4-trifluoro-1-(furan-2-yl)-3-(methylamino)but-2-en-1-yl)oxy)Lanthanum
4-M=Eu, L=Me
Tris(((Z)-4,4,4-trifluoro-1-(furan-2-yl)-3-(methylamino)but-2-en-1-yl)oxy)Europium

5-L=Ph
L1Ni

6-L=Me
L2Ni

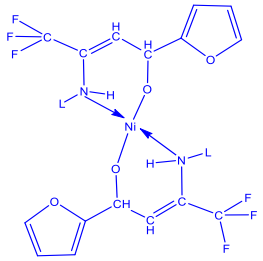

5-L=Ph
Bis(((Z)-4,4,4-trifluoro-1-1(furan-2-yl)-3-(phenylamino)but-2-en-1-yl)oxy)Nickel
6-L=Me
Bis(((Z)-4,4,4-trifluoro-1-1(furan-2-yl)-3-(methylamino)but-2-en-1-yl)oxy)Nickel

The proton nuclear magnetic resonance spectra ^{1}H NMR of the studied chemical compounds was measured using the Bruker-400MHz instrument, the first compound S (starting reagent) measured in a deuterated NMR solvent $CDCl_3$ where a peak appeared at (7.283 ppm) due to hydrogen residues in the Non-Deuterated CH group, while all other compounds were measured in the DMSO-d^6 solvent, the solvent shows two peak peaks at (2.560 ppm) due to the Non-Deuterated CH_3 group proton residues and a peak at (3.436 ppm) due to the proton residue in the water in the solvent. NMR spectra in all the studied compounds, when comparing the peak proton of the vinylic group between the ligand and the complex prepared from it, there is a generally upward shift at the proton peak site in the spectra, a clear indication of the occurrence of the reaction, also when comparing the peak location of the NH group proton between the ligand and the complex prepared from it (Moridi *et al*., 2025). It is observed that the proton peak site shifts towards the lower in a clear indication of the reaction on the one hand and the other hand, it shows that the Lone pair on the nitrogen atom was busy in the association (donate) with the metal, which weakened the withdrawal applied to the proton of the total NH as shown in Table 2 and Figures 1-6.

Table 2. ^{1}H NMR Data of compounds prepared

No.	Symbol of Comp.	CH_3	CH_2	$CH(SP^2)$	H(aromatic)	NH	OH
1	FTFA	---	3.311	6.494	6.619-7.687	---	13.934
2	FTLA	---	---	6.139	6.303-8.025	---	---
3	L1	---	2.434	6.080	6.431-8.024	11.594	---
4	L1La	---	---	6.096	6.416-8.692	11.536	---
5	L1Eu	---	---	5.908	6.303-7.712	10.164	---
6	L2	1.283 2.751	2.138	6.077	6.589-7.969	8.006	---
7	L2La	1.289	---	6.134	6.664-7.869	---	---
8	L2Eu	1.272	---	5.980	6.269-7.720	7.981	---

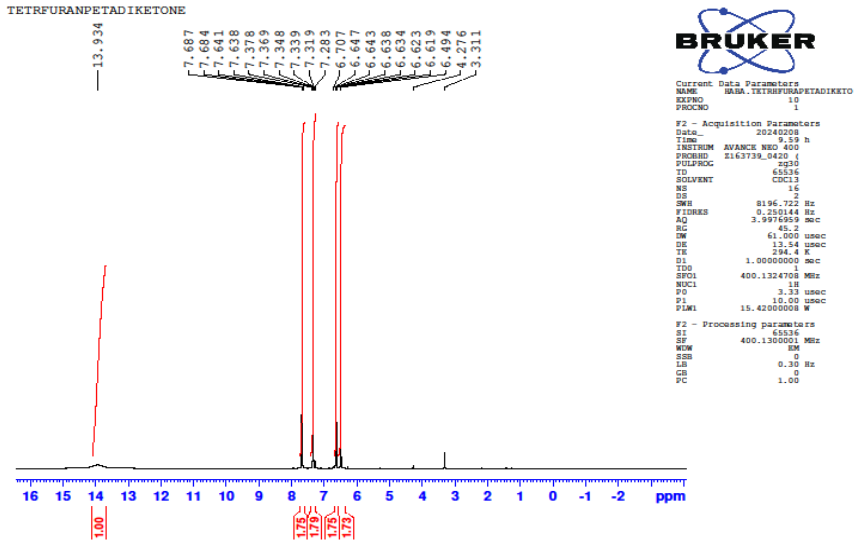

Figure 1. [1]H NMR spectrum of 4,4,4-trifloro-1-(2-furyl)-1,3-butanedione S compound

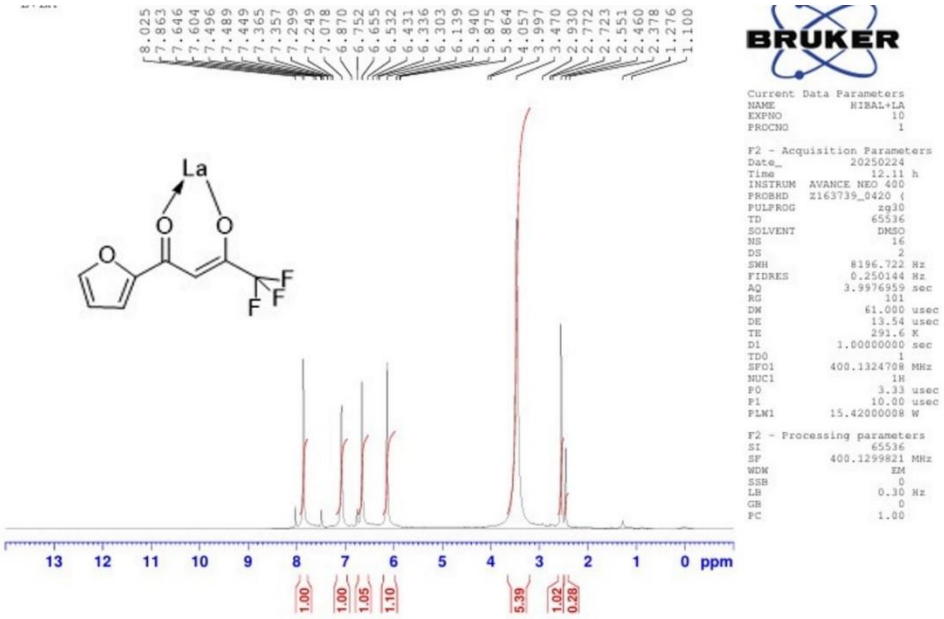

Figure 2. [1]H NMR spectrum of SLa compound

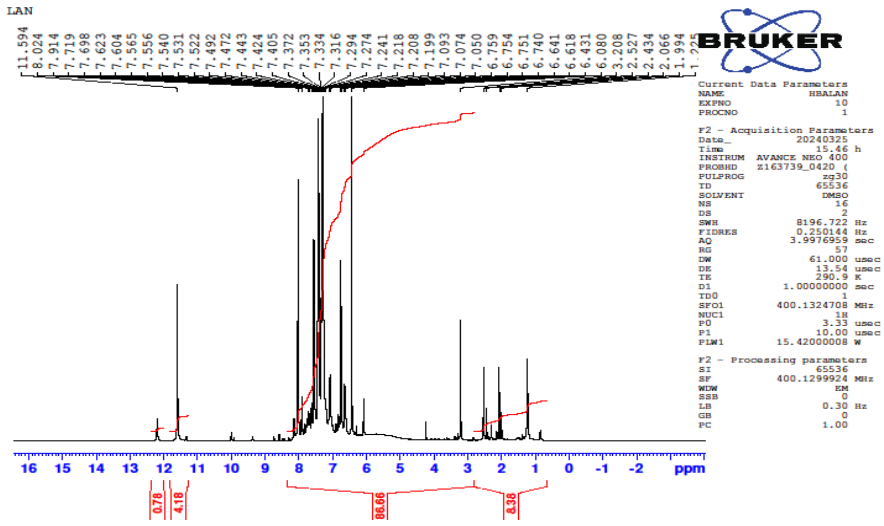

Figure 3. [1]H NMR spectrum of L1 compound

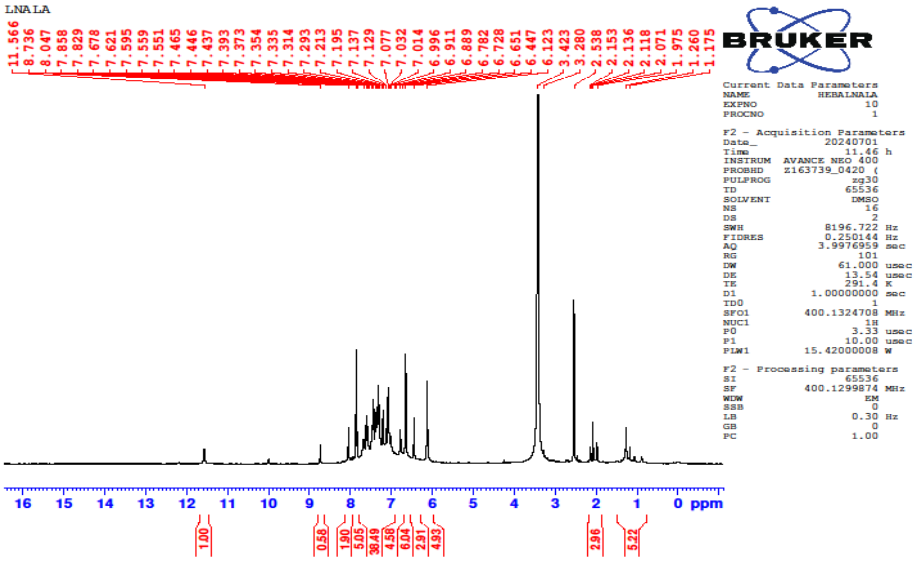

Figure 4. [1]H NMR spectrum of L1La compound

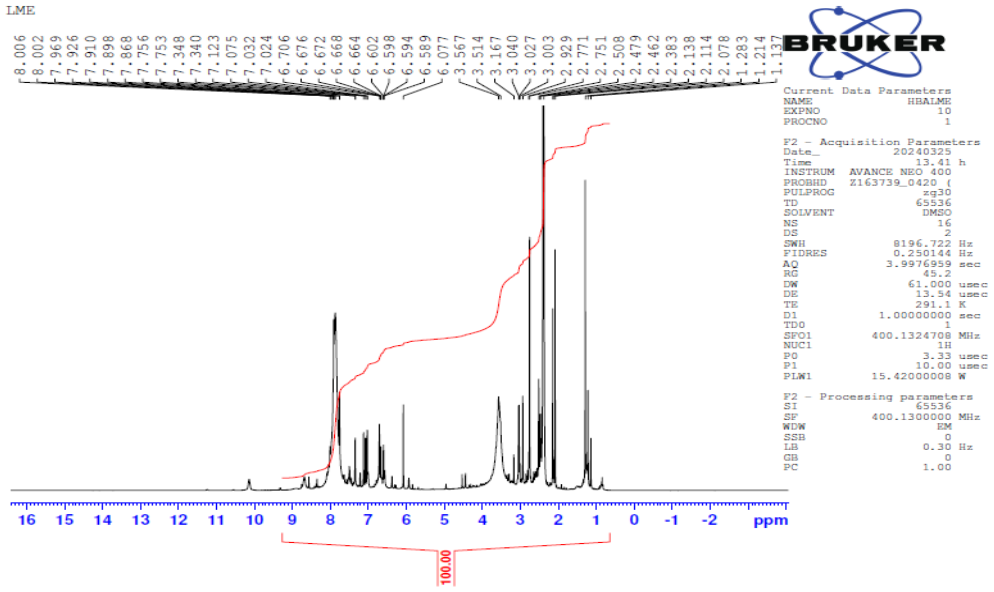

Figure 5. [1]H NMR spectrum of L2 compound

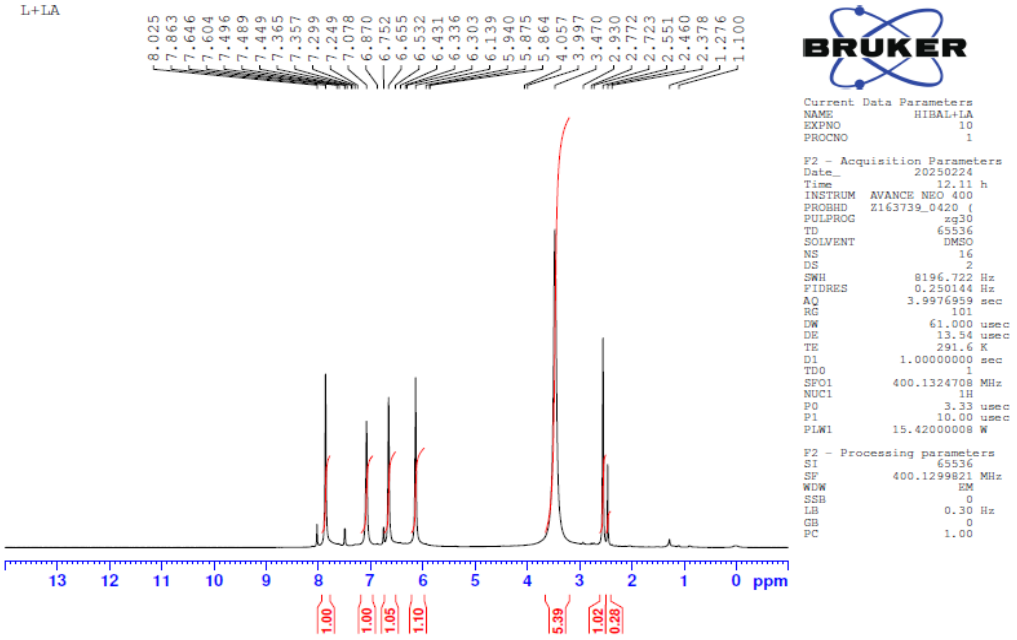

Figure 6. [1]H NMR spectrum of L2La compound

Measure the infrared spectrum of the compound L1, in which the band appears at (3307.57 cm^{-1}) due to the stretching vibration of the bond N-H, the compound L2 shows the absorption of the same group at (3429.01 cm^{-1}), while the absorption of the same group is observed in the prepared complexes at a higher wavenumber compared to the ligands prepared from them as an indication of the possibility of a back donation that occurs from the metal to the nitrogen atom, which leads to an increase in the bond strength constant N-H, which leads in turn to the absorption of the bond at a higher wavenumber of the ligands prepared from the complexes, the other significant absorption is at (1628.07 cm^{-1}) which is due to the stretching vibration of the group (C =O) of the compound L1

and at (1624.28 cm^{-1}) of the compound L2 while this absorption is observed disappears in the complexes to convert the group C=O to C-O It is known according to the literature that the group C=O shows a strong absorption characteristic in the I.R. spectrum of the polarity difference between the two atoms, another significant quartet absorption at the region (1095.24-1192.64 cm^{-1}) belongs to the CF_3 group of the compound L1 and at the area (1184.37-1115.75 cm^{-1}) for the L2 compound, where this region suffers a shift towards the upper or lower region Wavenumber in the prepared complexes is an indication of the reaction and transformation ligands to complexes (Pavia *et al*., 2015; Silverstein *et al*., 2017) as shown in Table 3 and Figures 7-14.

Table 3. FT.I.R. data for prepared compounds

N0.	N-H	C-H (aromatic)	C-H (Aliphatic)	C=O	C=C	C-O	C-N	CF_3
L1	3307.57	3135.42 3064.46	2925.83 2853.52	1628.07	1597.90	1304.83	1261.65	1192.64 1095.24
L1Ni	3390.86	3140.11 3059.10	2926.01 2854.65	---	1598.99	1319.31	1259.52	1168.86 1126.43
L1La	3363.86	3153.61	2960.73 2854.65	---	1616.35	1301.95	1257.59	1188.15 1095.57
L1Eu	3331.07	3122.75 3061.03	2960.73 2856.58	---	1595.13	1301.95	1259.52	1190.08 1095.57
L2	3429.01	3119.78	2974.49 2853.25	1624.28	1509.32	1303.65	1251.12	1184.37 1115.75
L2Ni	3431.36	3143.97	2958.80 2854.65	---	1608.63	1319.31	1261.45	1188.15 1130.29
L2La	3431.69	3150	2950	---	1624.71	1306.35	1259.41	1192.87 1098.03
L2Eu	3432.52	3150	2950	---	1624.36	1308.02	1259.20	1193.08 1099.91

The NMR spectra of the prepared compounds show a shift when comparing the enamine compounds prepared in the first step with the starting reagent prepared from it and a shift in the NMR spectra is also observed when comparing the complexes prepared in the second step with the enamine compounds prepared from it. This shifting in the NMR spectra confirms the expected reaction and the structure of the suggested compounds and improves the spectra are straightforward to diagnose in complexes because when bonding occurs in metal complexes stops the electronic transition of tautomeric and many isomers that occur through rotation that occurs in the synthetic formula of enamine compounds, which stops through bonding with the metal, which stops rotation in the isomers and stops the transfer of pi electrons that form the forms enol and ketone, in addition to the Lanthanide metals mainly working to separate the peaks in the NMR spectrum and facilitated by the diagnosis of NMR spectra, especially the metal Lanthanum, which forms diamagnetic when it loses three electrons in the complex prepared from it (Khalaf *et al*., 2025).

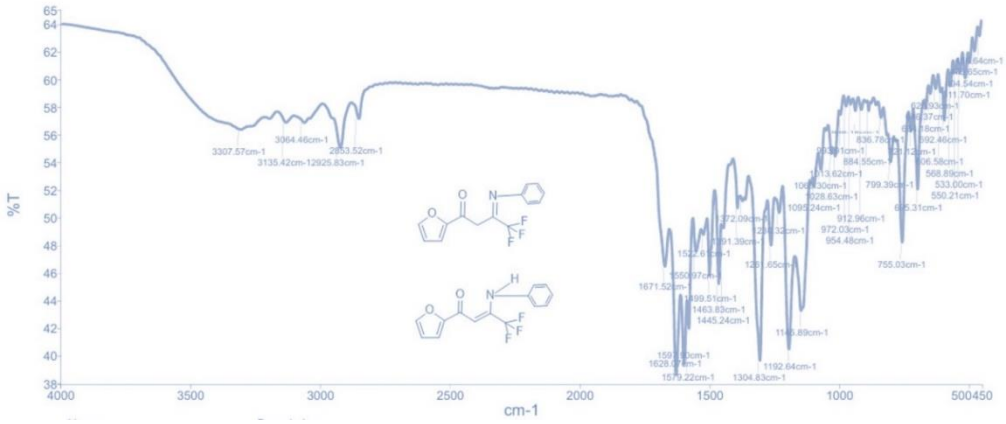

Figure 7. I.R spectrum of L1 compound

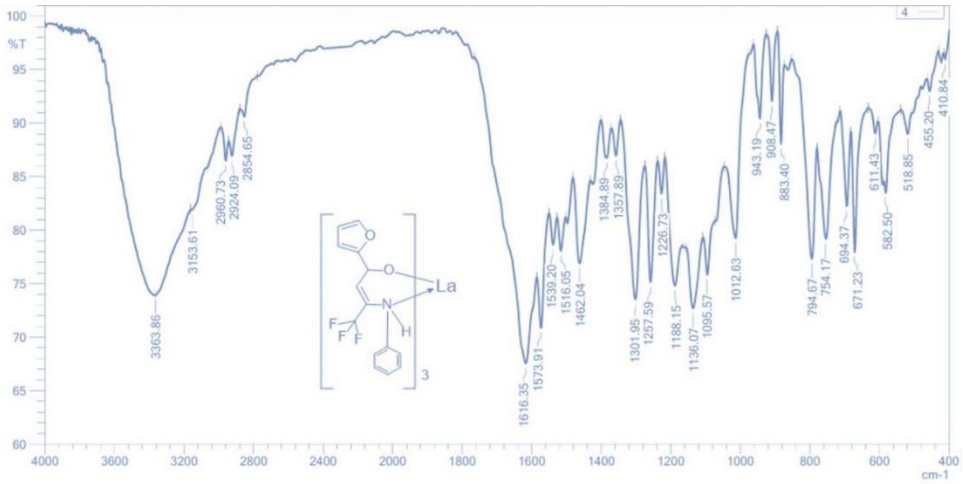

Figure 8. I.R. spectrum of L1La compound

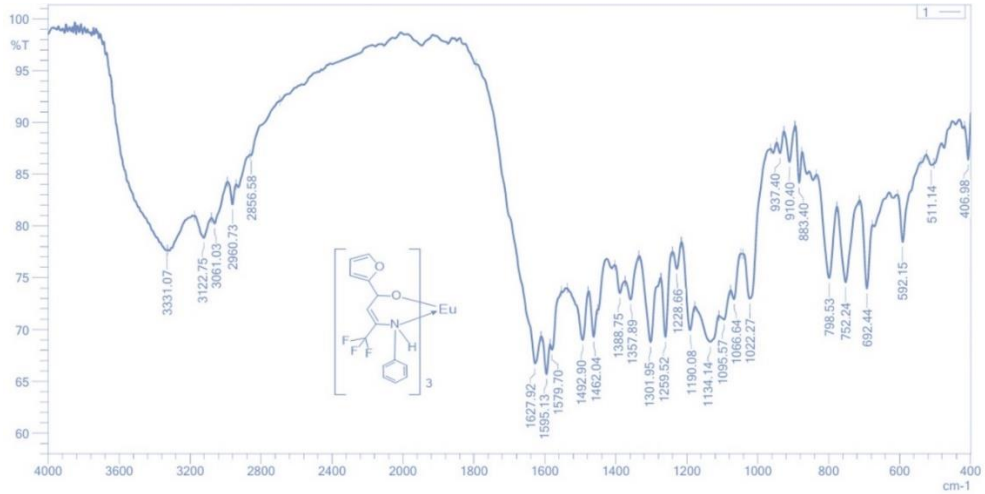

Figure 9. I.R. spectrum of L1Eu compound

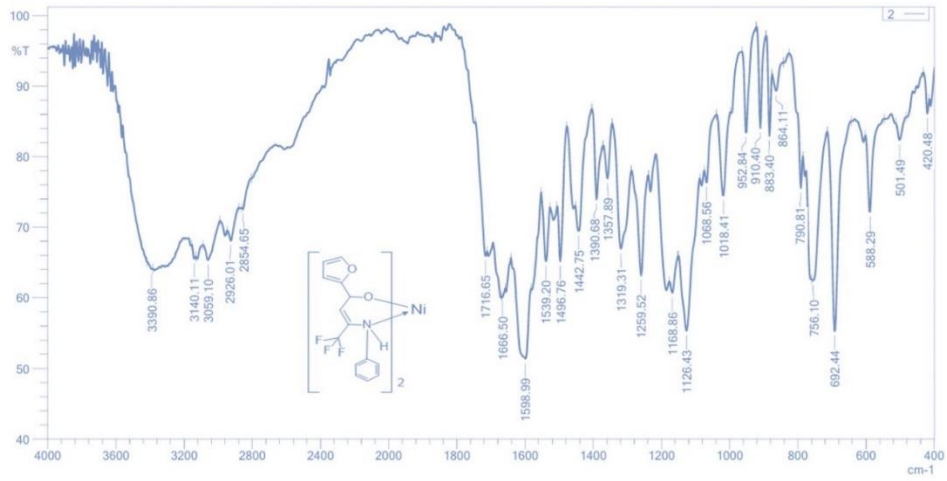

Figure 10. I.R. spectrum of L1Ni compound

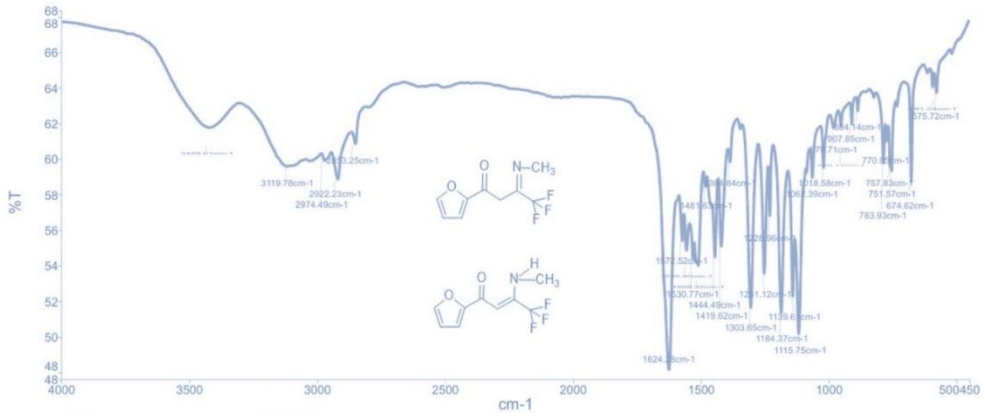

Figure 11. I.R. spectrum of L2 compound

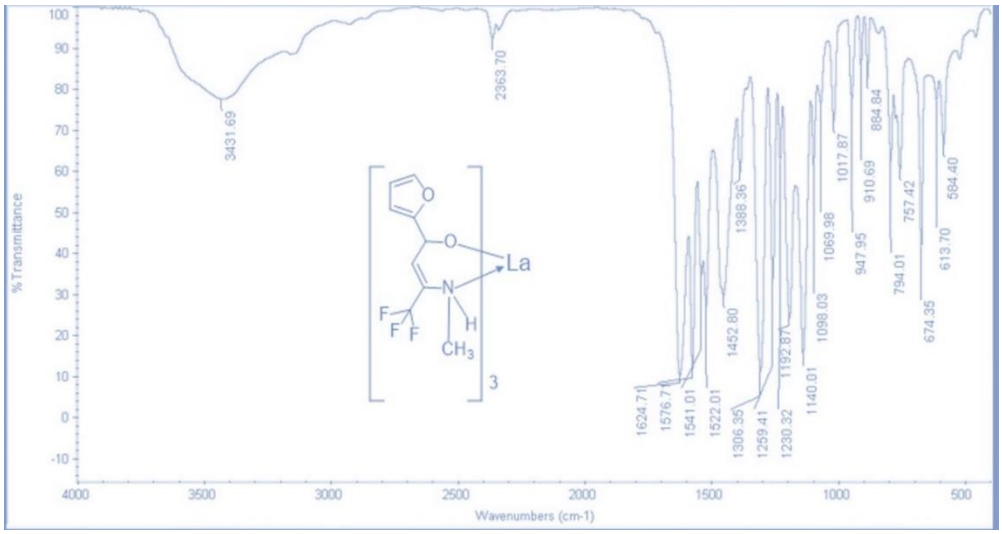

Figure 12. I.R. spectrum of L2La compound

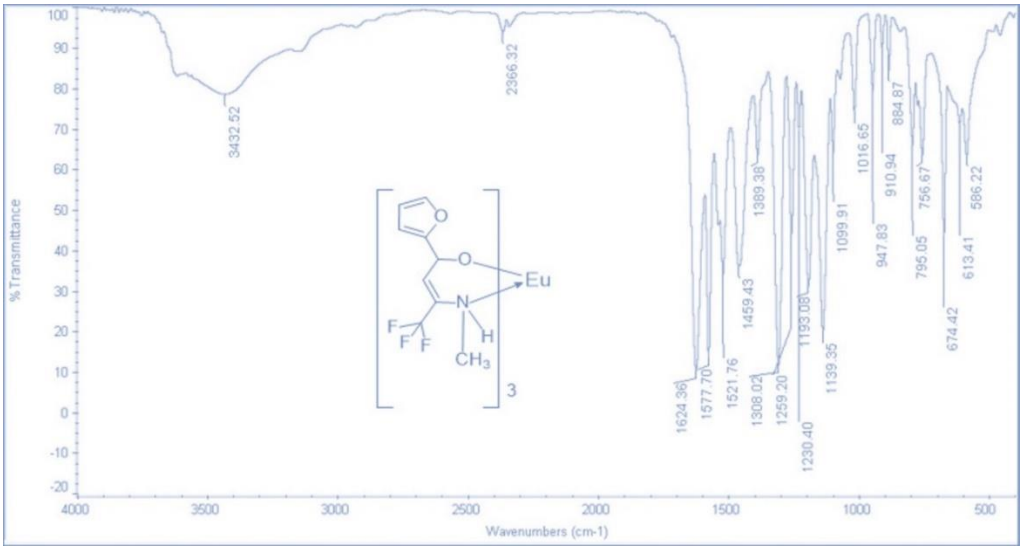

Figure 13. I.R. spectrum of L2Eu compound

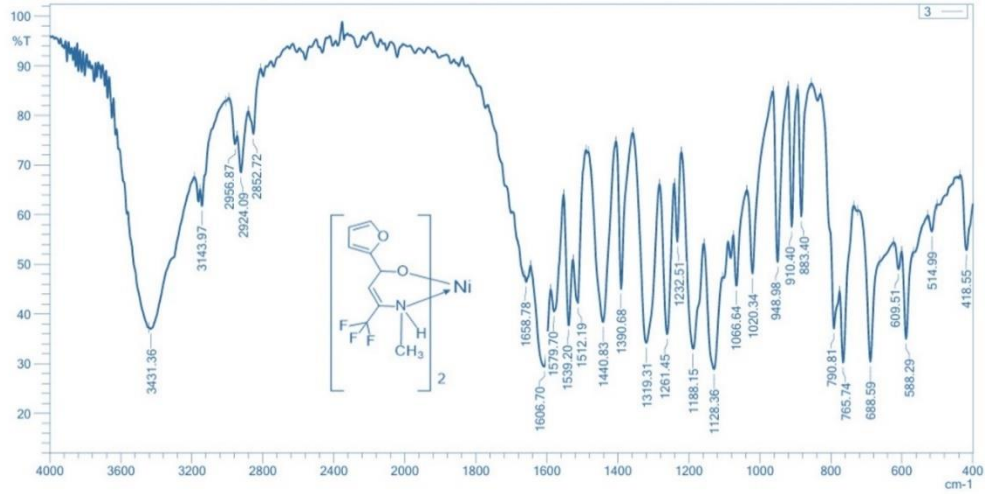

Figure 14. I.R. spectrum of L2Ni compound

The visible and ultraviolet spectra of enamine compounds and some complexes prepared from them were measured at different concentrations in ethanol solvent, except for the compound L2Eu dissolved in methanol and with a range of wavelengths of 200-800 nm, where the electron spectra appear within three regions that can be clarified as follows: Absorption beams within the range 224-245 nm and weak absorption peaks are formed due to n → σ* transitions electron transitions (Jima'a & Shaalandue, 2022) to the presence of sp^3 hybridization atoms containing electron lone pairs, which are not observed in the prepared complexes compared to the enamine compounds prepared from them. Absorption beams within the range 269-282 nm result from electronic transfers of the pi to the pi* operator type due to the presence of part of the aromatic compound and the presence of double bonds within the compound's chemical composition. These absorption beams are powerful in enamine compounds and turn into medium strength in complexes, which is clear evidence of the reaction and complex formation. Absorption beams within the range 334-340 nm due to n goes to pi to the asterisk operator electron transfers due to the presence of atoms with sp^2 hybridization within the aromatic medium. These

absorption beams are of medium strength in enamine compounds and become very strong in complexes as shown in Table 4 and Figure 15, which is clear evidence of reaction and complex formation (Jima'a & Shaalandue, 2022).

Table 4. UV-Visible data for some prepared compounds

compounds	Electronic Transition(nm)		
	$n \rightarrow \sigma^*$	$\pi \rightarrow \pi^*$	$n \rightarrow \pi^*$
L1	224	269	334
L2	225	269	336
L1La	243	281	337
L1Eu	243	282	338
L2Eu	225	282	340

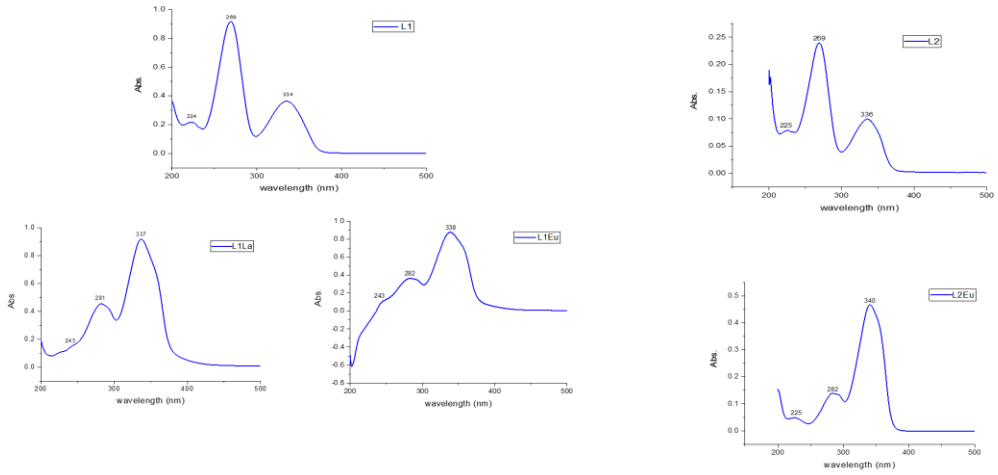

Figure 15. UV-Visible spectroscopy of prepared compounds

Molarity conductivity data (Tables 5 and 6) indicate that not all prepared complexes have extra-sphere ligands. After linking the molar conductivity data with the magnetic susceptibility data (Table 7) for all the prepared complexes, it became possible to propose chemical hybridization and thus know the geometric shapes of the prepared complexes, which indicate that hybridization in Ni^{+2} complexes is dsp^2. The shape is a square planar and hybridization in La^{+3} and Eu^{+3} complexes is d^2sp^3 and the shape is octahedral. From an application standpoint, the square-planar Ni(II) species exhibit σ→σ* shoulders around 225 nm that overlap with the actinic window commonly used in microfluidic chemotaxis platforms. Al-Abboodi et al. (2011) exploited a porous-gradient chip to interrogate nanoparticle-cell interactions; incorporating our Ni-enamine units as in-channel optical tracers would enable simultaneous gradient visualisation and catalytic quenching studies. Complementary evidence comes from ion-beam-sculpted hydrogels demonstrates that nanoscale patterning can embed catalytic and cell-adhesive domains directly inside microchannels (Kim *et al.*, 2014). Coupled with the design heuristics extracted via data-driven nanomaterial discovery (Hassan *et al.*, 2023), these findings chart a route toward AI-guided, lab-on-chip screening of photo-active coordination frameworks.

Table 5. Molar conductivity values of complex solutions prepared from the first ligand in the ethanol solvent

No.	Complex	molar conductivity (μs)	The ionic ratio
1	$[Ni(L1)_2]$	4.5	Non-Ionic
2	$[La(L1)_3]$	10.32	Non-Ionic
3	$[Eu(L1)_3]$	11.37	Non-Ionic

Table 6. Molar conductivity values of complex solutions prepared from the second ligand in the ethanol solvent

No.	Complex	molar conductivity (μs)	The ionic ratio
1	$[Ni(L2)_2]$	13.8	Non-Ionic
2	$[La(L2)_3]$	19.6	Non-Ionic
3	$[Eu(L2)_3]$	18.6	Non-Ionic

Table 7. Magnetic susceptibility data of prepared complexes

XA =XM+D

Magnetic effect M_{eff}(B.M)	Atomic susceptibility $\times 10^{-6}$	Diamagnetic corrections timD$\times 10^{-6}$	Mola susceptibility$X_M\times 10^{-6}$	Gramer susceptibility timesX$\times 10^{-6}$	complexes
0.93	372.79	-372.54	0.254674	4.1	$[Ni(L1)_2]$
1.15	561.63	-560.81	0.826402	8.3	$[Eu(L1)_3]$
0.78	256.34	-256.14	0.203776	4.1	$[Ni(L2)_2]$
0.95	386.88	-386.21	0.671846	8.3	$[Eu(L2)_3]$
0.00	0.00	0.00	0.00	0.00	$[La(L1)_3]$
0.00	0.00	0.00	0.00	0.00	$[La(L2)_3]$

4. Conclusion

In general, β-diketones exist in two forms, the keto and enol forms. Hover when the β-diketone is asymmetric, that is to say, the two carbonyl groups are adjacent to different chemical groups, CF_3 and furan. In this case, the enolization gives two other structures. In general, the enolization may occur adjacent to the CF_3 group. Therefore, one expects the compound to exist as a tautomeric form in the solution. The spectra show that enolic forms are dominant. All complexes prepared do not contain an ionic outside coordination sphere. The hybrid of the complexes prepared is d^2sp^3 of complexes prepared from lanthanide and dsp^2 of complexes prepared from Ni.

References

Al-Abboodi, A., Tjeung, R., Doran, P., Yeo, L., Friend, J. & Chan, P. (2011). Microfluidic chip containing porous gradient for chemotaxis study. In *Smart Nano-Micro Materials and Devices*, 8204, 219-224.

Aldujaili, N.H., Banoon, S.R. (2020). Antibacterial characterisation of titanium nanoparticles nanosynthesised by Streptococcus thermophilus. *Periódico Tchê Química, 17*(34), 311-320.

AlHasan, L., Qi, A., Al-Aboodi, A., Rezk, A., Shilton, R.R., Chan, P.P., ... & Yeo, L. (2013). Surface acoustic streaming in microfluidic system for rapid multicellular tumor spheroids generation. *Micro/Nano Materials, Devices and Systems*, 8923, 828-831.

AL-Hilfi, J.A. (2020). A structural study of 2-thenoyltrifluoroacetone Schiff bases and their thione derivatives: Synthesis, NMR and IR. In *AIP Conference Proceedings*, 2290, 030030. https://doi.org/10.1063/5.0027547

AL-Hilfi, J.A., Abood, N., Fahad, T.A. & Turner, S. (2015). Synthesis and structural study of some new metal complexes of Schiff base from 2-thenoyltrifluoroacetone with alkyl amine and its thione derivative by NMR, IR and TGA analysis methods. *Pelagia Research Library*, *6*(11), 37-41.

AL-Hilfi, J.A., Kahdim, Z.J., Fandi, T.S. & Ahmed, L.M. (2020). Structural study of complexes from hexafluoroacetylacetone, pyrazole and its derivative with some metals by FT-IR and ^{1}H-NMR. *Periódico Tchê Química*, *17*(34), 756-768.

Ali, Z.H., Al-Saady, M.A.A.J., Aldujaili, N.H., & Banoon, S.R. (2020). Evaluation of the antibacterial inhibitory activity of chitosan nanoparticles biosynthesised by Streptococcus thermophilus. *Journal of Nanostructures*, 12, 675-685.

Arrachart, G., Couturier, J., Dourdain, S., Levard, C. & Pellet-Rostaing, S. (2021). Recovery of rare earth elements (REEs) using ionic solvents. *Processes*, *9*(7), 1202.

Aziz, Z.S., Jazaa, S.H., Dageem, H.N., Banoon, S.R. & Balboul, B.A. (2024). Bacterial biodegradation of oil-contaminated soil for pollutant abatement contributing to achieve sustainable development goals: A comprehensive review. *Results in Engineering*, 102083.

Banoon, S.R., Ghasemian, A. (2022). The characters of graphene oxide nanoparticles and doxorubicin against HCT-116 colorectal cancer cells in vitro. *Journal of Gastrointestinal Cancer*, 53, 410-414.

Banoon, Z.R., Al-Lami, A.K.A. & Abbas, A.M. (2023a). Asymmetric dimeric liquid crystals and their application as fluorescence and nanohybrid: A review. *Journal of Nanostructures*, *13*(1), 274-295.

Banoon, Z.R., Al-Lami, A.K.A. & Abbas, A.M. (2023b). Synthesis and studying the optical properties of novel zinc oxide/a symmetric dimer liquid crystal nanohybrid. *Journal of Nanostructures*, *13*(1), 159-172.

Hanson, D. (2014). Synthesis and thermodynamic analysis of volatile beta-diketone complexes of select lanthanides via gas-phase separations. Doctoral dissertation, University of Tennessee, Knoxville.

Hassan, S.A.D.H., Almaliki, M.N.S., Hussein, Z.A., Albehadili, H.M., Rabeea Banoon, S., Abboodi, A. & Al-Saady, M. (2023). Development of nanotechnology by artificial intelligence: A comprehensive review. *Journal of Nanostructures*, *13*(4), 915-932.

Jima'a, R.B., Shaalan, N.D. (2022). Synthesis, characterization and biological activity of new metal ion complexes with Schiff base derived from 2-acetylthiophene and isatin. *Egyptian Journal of Chemistry*, *65*(132), 1409-1419.

Khalaf, R.N., Hassan, A.I., El-Shafiey, Z.A., Faheim, A.A., Ibrahim, S.S. & Saleh, H.M. (2025). Evaluation of an isatin-derived ligand and its metal complexes as potential anticancer agents in breast adenocarcinoma cells. *Chemical Papers*, 79(3), 1539-1560.

Kim, Y., Abuelfilat, A.Y., Hoo, S.P., Al-Abboodi, A., Liu, B., Ng, T., ... & Fu, J. (2014). Tuning the surface properties of hydrogel at the nanoscale with focused ion irradiation. *Soft Matter*, *10*(42), 8448-8456.

Mautner, F.A., Bierbaumer, F., Vicente, R., Speed, S., Tubau, Á., Fischer, R.C., & Massoud, S.S. (2022). Magnetic and luminescence properties of 8-coordinated pyridyl adducts of samarium (III) complexes containing 4, 4, 4-trifluoro-1-(naphthalen-2-yl)-1, 3-butanedionate. *Magnetochemistry*, *8*(7), 72. https://doi.org/10.3390/magnetochemistry8070072

Moridi, H., Behroozikhah, H., Talebi, M., Mousavi, S.E. & Abbasizadeh, S. (2025). Fabrication of a chitosan-grafted-4-vinylpyridine/thiol-amine-HZSM-5 nanocomposite via casting method in adsorption of heavy cations from water systems: An evaluation of adsorption mechanism. *Environmental Science and Pollution Research*, *32*(11), 6628-6657.

Omoregie, H.O. (2018). Synthesis, physicochemical properties and antimicrobial activities of nickel (II) complexes of 4, 4, 4-trifluoro-1-(2-naphthyl)-1, 3-butanedione and their adducts. *International Journal of Chemistry*, *10*(4), 1. https://doi.org/10.5539/ijc. v10n4p1

Pavia, D.L., Lampman, G.M., Kriz, G.S. & Vyvyan, J.R. (2015). *Introduction to Spectroscopy*. Cengage Learning.

Petrova, E.M.A. (2022). Synergistic solvent extraction of lanthanoids using a combination of chelating and organophosphorus ligands: From ancient beginnings to modern scientific chefs-d'oeuvre. Doctoral dissertation, University of Chemical Technology and Metallurgy.

Saleh, H., Al-Kahlidi, M., Abulridha, H.A., Banoon, S.R. & Abdelzaher, M.A. (2021). Current situation and future prospects for plastic waste in maysan governorate: Effects and treatment during the COVID-19 pandemic. *Egyptian Journal of Chemistry*, *64*(8), 4449-4460.

Silverstein, R.M., Webster, F.X., Kiemle, D.J. & Bryce, D.L. (2017). *Spectrometric Identification of Organic Compounds*. John Wiley & Sons, 495.

Taydakov, I.V., Belousov, Y.A., Metlin, M.T. & Gontcharenko, V.E. (2022). (Diaqua) hexakis (4, 4, 4-trifluoro-1-(1-methyl-1 H-pyrazol-4-yl) butane-1, 3-dionato-κ2O, O')(μ-(1, 4-dioxane)) digadolinium (III), solvate with two molecules of 1, 4-dioxane. *Molbank*, *2022*(4), M1452. https://doi.org/10.3390/m1452